between the theory and the experiment noticed in the earlier investigations.

4) The pylon damping in the absence of flap damping does not have much influence on the flutter speed in the rotors with hinge offset blades unlike in prop-rotor with rigidly connected blades. However, in the presence of flap damping the pylon, damping has a stabilizing effect. The flap damping might reduce the backward flutter speed and may even change the predominant flutter speed from backward to forward.

5) The divergence speed of the system decreases with an increase in coning angle.

6) The coning angle β_0 is small for windmilling case of the propeller. However, in view of its marked effect on stability depending on other parameters the analytical results without considering it may lead to wrong conclusions.

References

[1] Richardson, J. R. and Naylor, H. F. W., "Whirl flutter of Propellers with Hinged Blades," Rept. No. 24, March 1962, Engineering Research Associates, Toronto, Canada.

[2] Reed, W. H., III and Bennett, Robert, M., "Propeller Whirl Flutter Considerations for V/STOL Aircraft," *Cal/Trecom Symposium Proceedings*, Vol. II. *Dynamic Load Problems Associated with Helicopters and V/STOL Aircraft*, June 1963, Cornell Aeronautical Lab., Buffalo, N.Y.

[3] Reed, W. H., III, "Propeller-Rotor Whirl Flutter: A State of the Review," *Journal of Sound and Vibrations*, Vol. 4, No. 3, 1966, Pages 526–544.

[4] Reed, W. H., III, "Review of the Propeller-Rotor Whirl Flutter," TR R-264, July 1967, NASA.

[5] Young, M. I. and Lytwyn, R. T., "The Influence of Blade Flapping Restraint on the Dynamic Instability of Low Disc Loading Propeller-Rotors," *Journal of American Helicopter Society*, Vol. 12, Oct. 1967.

[6] Kaza, K. R. V. and Sundararadan, D., "Whirl Flutter of Flapped Blade Rotor Systems," TN-18, Oct. 1969, National Aeronautical Laboratory, Bangalore, India.

[7] Loewy, R. G., "Review of Rotory-Wing V/STOL Dynamic and Aeroelastic Problems," *AIAA/AHS VTOL Research Design and Operations Meeting*, Georgia Institute of Technology, Vol. 14, Feb. 1969.

[8] Ziegler, H., *Principles of Structural Stability*, Blaisdell Publishing Co., Mass., June 1966, pp. 93–96.

[9] Terndrup P. P., "On Forward and Backward Precission of Rotors," Rept. No. 17, Sept. 1971, The Technical University of Denmark, Lyngby, Denmark.

NOVEMBER 1973 J. AIRCRAFT VOL. 10, NO. 11

Active Flutter Control—An Adaptable Application to Wing/Store Flutter

William E. Triplett,* Hans-Peter F. Kappus,† and Robert J. Landy‡
McDonnell Aircraft Company, St. Louis, Mo.

An active flutter suppression system using an electronically compensated feedback signal can be adapted to stabilize widely differing wing/store flutter mechanisms. A generalized compensation network in the feedback loop modifying the signal of a single wing motion sensor is shown to provide sizable stability margins out to the aircraft performance limits for several airplane/store configurations. Flutter control can be maintained even though aileron actuators are rate saturated during flutter suppression. Usual levels of hydraulic system deadspace and freeplay do not impair the suppression system operation. Necessary hardware improvements include: increasing component reliabilities, increasing hydraulic flow rate, and improving actuator bandwidths.

Introduction

MILITARY aircraft are subjected to significant velocity restrictions when operating with external stores. A current fighter, for example, is restricted by flutter considerations to speeds below 550 KEAS (Knots Equivalent Air Speed) for several store configurations, even though the maximum velocity of the airplane is significantly greater. The ability to use the full velocity envelope while carrying external stores could enhance aircraft survivability with respect to ground fire and pursuing enemy interceptors. In addition the removal of flutter placards could improve bombing accuracy and effectiveness by lowering the minimum safe release altitude. Active flutter control, a concept using a feedback signal to actuate a control surface and eliminate the aeroelastic instability, is one means of removing flutter placards.

The feasibility of active control of wing/store flutter was previously established[1] on the basis of linear analyses of one wing/store configuration with a 370 gal fuel tank 90% full on the outboard store station. Those studies were the first steps in the design of an active flutter control system for wing/store flutter.

This paper reports on the results of an Air Force contract[2] which significantly expanded the scope of the previous studies to include the evaluation of 1) the ability of a single scheme to control flutter for several configurations; 2) the effects of system nonlinearities and equipment limitations; 3) the changes in aircraft stability resulting from the integration of the flutter suppression scheme into the existing aircraft flight control system; and 4) the system redundancy to satisfy flight safety requirements. Additional Air Force efforts in the area of flutter suppression are described in Refs. 3 and 4.

Four separate wing/store configurations, chosen to cover a broad spectrum of possible configurations, are presented. The general results obtained are believed to be applicable to most of the wing/store flutter mechanisms encountered on other low-to-moderate aspect ratio fighter/bombers.

Presented as Paper 73-194 at the AIAA 11th Aerospace Sciences Meeting, Washington, D.C., January 10–12, 1973; submitted March 1, 1973; revision received August 30, 1973. Work sponsored by the Air Force Flight Dynamics Laboratory, Wright-Patterson Air Force Base, Ohio, under Contract F33615-71-C-1481.

Index categories: Structural Dynamic Analysis; Aircraft Handling, Stability and Control.

*Senior Technical Specialist, Structural Dynamics. Associate Fellow AIAA.

†Engineer, Structural Dynamics.

‡Group Engineer, Guidance and Control Mechanics.

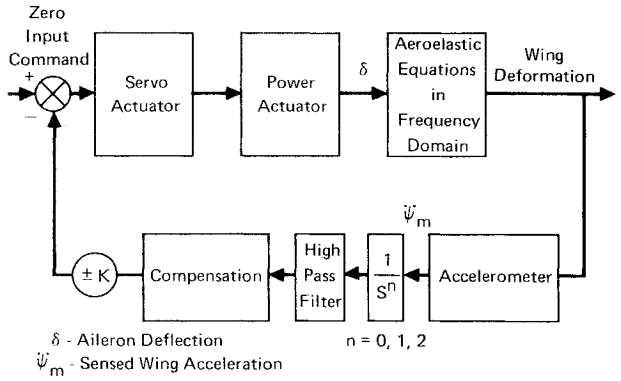

Fig. 1 Block diagram showing generalized active flutter control loop.

Digital computer programs for integrated control-structural dynamic analyses have been used in these studies. The programs, which are described in Ref. 1, evaluate the dynamic stability of a general aeroelastic system considered as an integral part of a multi-loop feedback control system.

Active Flutter Control Scheme

In general there are three functions which an active flutter control scheme must perform: sensing of the flutter mode, compensation of the feedback signal, and control force production.

The flutter mode can be sensed by transducers which generate either an electrical signal or a physical displacement. Feedback compensation can also be accomplished by either electrical or mechanical components. Control forces for wing/store flutter control systems can be produced either by inducing a cyclically varying moment about the wing or by actually decoupling the store vibratory motion from that of the wing.

The scheme which is most easily adapted to a change in store carriage uses an existing lateral control system with an electronically compensated accelerometer signal in the feedback loop. A change in store carriage can be accommodated by making an adjustment in the electronic compensation. A functional block diagram of this flutter control scheme, which is identical to the scheme used in Ref. 1, is shown in Fig. 1. With compensation, the system will continuously oppose the wing deformation at the accelerometer location through aileron actuation. Existing aircraft hydraulic components make up the system forward loop. These include the aileron power actuator, an electrically commanded hydraulic servo-actuator to move the control valve of the actuator, and the aircraft structural

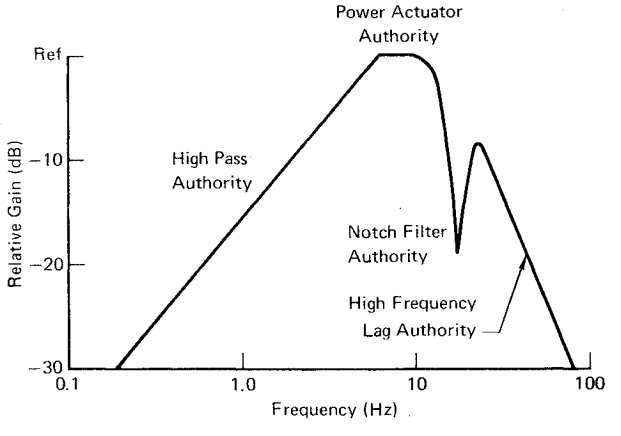

Fig. 2 Typical open loop Bode gain diagram for general active flutter control scheme.

Table 1 Summary of Store Properties

Configuration	Mass Mugs	I Pitch[c] Mug-in.^{2}	I Yaw[c] Mug-in.^{2}	I Roll[c] Mug-in.^{2}
370 gal. Fuel Tank [a]	6.507	12947.2	18180.0	507.0
90% Full	4.737	5003.0	6444.0	412.0
62% Full				
2000 lb Bomb, Max Weight-Min Inertia-Fwd CG	6.086	5642.5	5642.5	291.6
500 lb Bombs[b] Rack Locations 3 and 4	3.321	7950.0	7974.0	90.9

Notes: a. Fuel Assumed to be Liquid.
b. Bombs 3 and 4 in Combination with Rack Treated as one Store. Totals for the Combination.
c. All Inertias are Referenced to Store CG. (Mug = lb sec^2/in.)

transfer function which defines the wing deformation caused by an aileron deflection.

The feedback loop consists of an accelerometer, possibly a single or double integrator, electronic compensation elements, and a high pass filter. Since the aileron is shared by both the lateral control and flutter control systems the high pass filter must be incorporated to decouple the two systems. Without this decoupling the flutter control system would continuously counteract the pilot's commands by reacting to pilot induced wing deformations. Fortunately, the wing/store flutter frequencies studied are sufficiently high (greater than 7 Hz) so that the response of the flutter control system can be attenuated at low frequencies without compromising its ability. Aircraft with more flexible, larger aspect ratio wings may require separate dedicated control surfaces for active flutter control.

Study Configurations

Mass and Inertia Properties

Many aircraft carry a large number of different stores exhibiting a variety of dynamic properties and flutter mechanisms. The number of possible combinations is in the millions. Instances of mild wing/store flutter have been documented during flight testing and several stores are currently subject to flutter velocity placards. The stores examined in this study are: the 370 gal external fuel tank—90% and 62% full, a 2000 lb bomb, and 500 lb general purpose bombs carried on an ejection rack.

The diverse mass and inertia characteristics of this set of stores are listed in Table 1. Because of the wide variation in these properties, the general trends determined for these stores should be applicable to most wing/store flutter mechanisms encountered on contemporary fighter/bombers.

370 gal Fuel Tank

The 90% full configuration was selected for analysis because it is a flight-verified minimum flutter velocity case. The 62% full case was included to get a complete picture of how changing inertia and mass characteristics affect the ability to control flutter. The 62% full case occurs when the fore and aft sections of the three compartment tanks are empty. The pitch inertia values given in the table have been adjusted to account for fuel slosh effects.

2000 lb Bomb

The store characteristics given in the table correspond to the maximum weight, minimum pitch inertia, and most forward center of gravity normally encountered in

Table 2 Summary of Wing/Store Flutter Analyses

Configuration	M = 0.9 Analysis using C_{L_α} = 4.6, CP at 25% Chord			M = 1.2 Analysis using C_{L_α} = 4.08, CP at 37% Chord		
	Flutter Velocity (KEAS)	Freq. (Hz)	g/v (1/100 KEAS)	Flutter Velocity (KEAS)	Freq. (Hz)	g/v (1/100 KEAS)
370 gal Tank 90% Full	600	8.33	0.051	621	8.45	0.047
370 gal Tank 62% Full	713	10.13	0.042	987	10.09	0.032
2000 lb Bomb	683	10.71	0.024	731	11.09	0.0082
500 lb Bombs	371	7.67	0.0078	377	7.67	0.0064

production versions of the bomb. This particular combination of bomb properties results in a minimum flutter onset velocity.

500 lb Bombs

Up to six 500 lb general purpose bombs can be carried on each wing. The bombs are carried in clusters of three in fore and aft positions on an armament rack. The specific configuration analyzed was with two bombs only: the inboard shoulder bombs in the fore and aft clusters. This configuration occurs on the left wing during the normal release sequence whenever a full load is carried. This configuration, again, is the most flutter critical.

Passive Flutter Studies

The analytical model for each wing/store configuration consists of a truncated set of 10 normal modes for the aircraft wing, based on measured inertia data and structural influence coefficients. The critical flutter mode in all of the cases is symmetrical, so the effect of rigid motion of the aircraft in translation and pitch is incorporated into the normal mode vibration analysis.

Modified strip theory aerodynamics with experimental coefficients were used in the analysis. An indicial lift formulation[5] of the flutter equations was used to determine passive flutter velocities and mechanisms. Wind tunnel test data[6] were used to obtain values for the lift curve slope $C_{L\alpha}$ and center of pressure (CP) location. Two aerodynamic conditions were chosen for the study: Mach = 0.9, $C_{L\alpha}$ = 4.6/rad, CP = 25% chord, and Mach = 1.2, $C_{L\alpha}$ = 4.08/rad, CP = 37% chord. The two Mach number conditions were chosen to encompass the region of the flight envelope in which wing/store flutter normally occurs.

A summary of the flutter onset data for each of the study configurations is given in Table 2. The columns labeled g/v give the change in effective structural damping coefficient during a 100 knot velocity increment centered at the flutter onset velocity. This parameter is a measure of the severity of flutter: the larger value, the more explosive the flutter. The table shows that in every instance supersonic aerodynamics increase the flutter onset velocity. Each primary flutter mechanism involves coalescence of the 2nd and 3rd still air modes, regardless of the aerodynamics used.

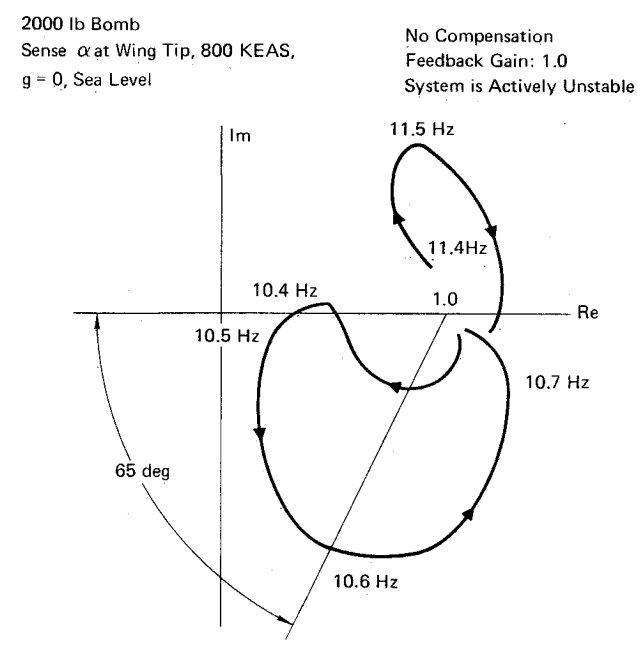

Fig. 3a Nyquist plot for the 2000 lb bomb, uncompensated.

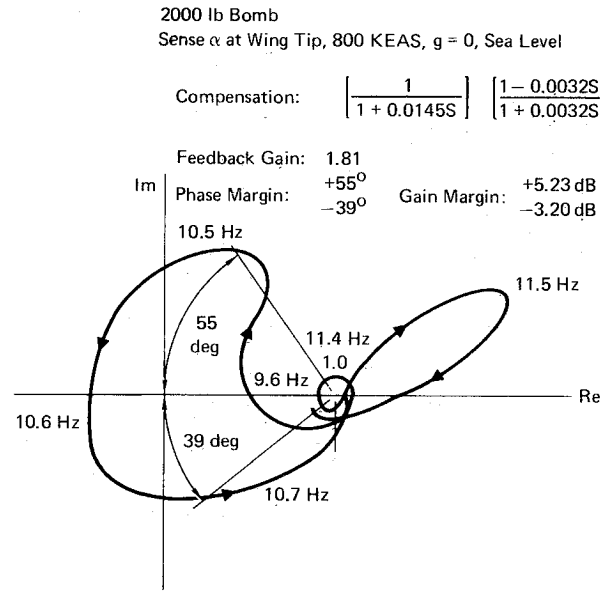

Fig. 3b Nyquist plot for the 2000 lb bomb, compensated.

Control System Design Studies

System Gain Characteristics

The philosophy used in planning an active flutter control system is to maximize the open loop gain at the flutter frequencies while minimizing it at all other frequencies. The desired open loop Bode gain diagram for an active flutter control system which shares the forward loop with the aircraft lateral control system is shown in Fig. 2. The actual control of the flutter mode is achieved through phase stabilization. The high pass filter causes the 20 dB/decade gain buildup and the low frequency break at the maximum gain "plateau" as shown in the figure. The high frequency break of the "plateau" is caused by the combined effects of the aileron actuator, a notch filter, and a first order, high frequency lag term. The frequency borders of the maximum gain "plateau" closely coincide with the expected frequency range of flutter to be controlled. Typical wing/store configurations have flutter frequencies ranging between 7 and 11 Hz. The high pass filter and aileron actuator transfer functions selected to

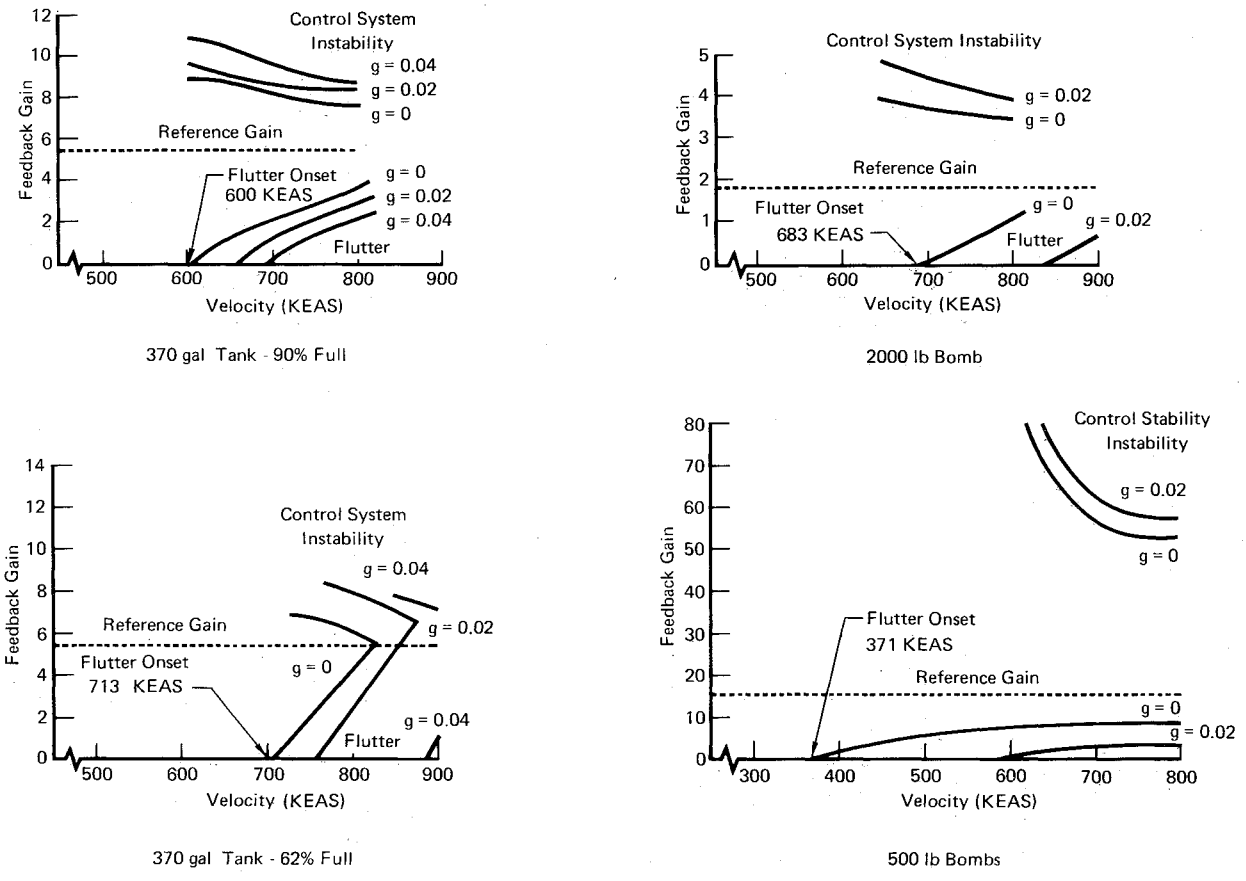

Fig. 4 Range of stable gain values for compensated wing/store configurations—subsonic data.

bracket these frequencies are

$$\text{High Pass Filter (6 Hz Break)} \quad \frac{0.0265S}{1 + 0.0265S}$$

$$\text{Aileron Power Actuator (10 Hz Break)} \quad \frac{1}{1 + 0.016S}$$

The 10 Hz break represents a significant improvement over the existing actuator, which has a break frequency of 1.6 Hz.

The notch filter indicated on the Bode diagram prevents the system from reacting to stable structural resonances which are within several Hertz of the flutter frequency. The high frequency lag assists the notch filter, attenuates the higher mode structural resonances, and also minimizes the effect of the resonances of the servo-actuator and the accelerometer. The transfer functions used for these elements are

$$\text{Servo-actuator (36 Hz Resonance)} \quad \frac{1}{1 + [2(0.86)/226]S + S^2/(226)^2}$$

$$\text{Accelerometer (80 Hz Resonance)} \quad \frac{1}{1 + [2(0.6)/502]S + S^2/(502)^2}$$

The servo-actuator transfer function matches the characteristics of the quadruply redundant servo-actuator on the Survivable Flight Control System (SFCS)[7] aircraft lateral control system. This SFCS actuator was used, rather than the production servo-actuator because it is well over one million times as reliable.

For the wing/store configurations considered in these studies it was necessary to integrate the accelerometer output twice in order to prevent a control system instability at the servo-actuator resonance, 36 Hz.

Compensation Design

The complete generalized compensation used in these studies is given below with a summary of the function of each element

$$\pm K\left[\frac{1 - \tau_2 S}{1 + \tau_2 S}\right]\left[\frac{\omega_N^2 + 2\omega_N\zeta_N S + S^2}{\omega_D^2 + 2\omega_D\zeta_D S + S^2}\right]\left[\frac{1}{1 + \tau_3 S}\right]$$

Phase Lag Network	Notch Filter	High Frequency Lag

Phase Lag Network —gives required phase lag for stability with no gain reduction

Notch Filter —gain stabilizes non-flutter modes which occur at frequencies near the flutter frequency

High Frequency Lag —gain stabilizes non-flutter resonances far removed from the flutter frequency

The sign on the feedback gain, K, can be adjusted to ensure that the system can be phase lag compensated. Some of the phase lag compensation is achieved with the notch filter and high frequency lag term. However, the prime flutter mode stabilizer in the compensation is the pure phase lag network. It is ideal for this application since large phase lag compensations can be introduced at a constant gain.

The effect of adding the compensation elements to the feedback loop of a flutter control system is illustrated by the system Nyquist plots in Fig. 3. Figure 3a shows the 2000 lb bomb configuration without compensation while the Fig. 3b has compensation added. The Nyquist plots are modified from the classical form in that +1 has been

added to all the frequency data points. The origin thus becomes the critical point.

An open loop pole in the right half complex plane (flutter mode) is indicated by a counter-clockwise loop. For system stability the Nyquist criterion states that this loop must encircle the critical point. These conditions are met in Fig. 3b. Encirclements of the origin by clockwise loops must be precluded since this indicates a control system instability.

The compensations for each of the study configurations are listed below

Pure Phase Lag	Notch Filter	High Frequency Lag
	370 gal tank 90% full	
$-5.34\left[\frac{1-0.029S}{1+0.029S}\right]$	(No Notch Req'd)	$\left[\frac{1}{1+0.0177S}\right]$
	370 gal tank 62% full	
$+5.46\left[\frac{1-0.242S}{1+0.242S}\right]$	$\left[\frac{122.5^2+2(0.1)(122.5)S+S^2}{122.5^2+2(0.7)(122.5)S+S^2}\right]$	$\left[\frac{1}{1+0.0133S}\right]$
	2000 lb Bomb	
$+1.81\left[\frac{1-0.0032S}{1+0.0032S}\right]$	(No Notch Req'd)	$\left[\frac{1}{1+0.0145S}\right]$
	500 lb Bombs	
$+15.21\left[\frac{1-0.124S}{1+0.124S}\right]$	$\left[\frac{100^2+2(0.1)(100)S+S^2}{100^2+2(0.7)(100)S+S^2}\right]$	$\left[\frac{1}{1+0.0177S}\right]$

These compensations were selected to yield approximately balanced phase margins at 800 knots, sea level, zero structural damping conditions. Gain margins, defining the maximum feedback gains which still allow encirclement of the Nyquist critical point by the flutter mode loop, are affected by the selection of feedback gain and notch filter position. The maximum phase margins, which are dependent on the angular size of the unstable loop, cannot be significantly affected by the compensation elements because of the rapid frequency variation around the loop. The sensor location, however, can affect the maximum phase margins. The response at any location is the weighted summation of each generalized coordinate response at the sensor location. From the flutter control standpoint it is desirable to detect the maximum unstable mode contribution to the maximum exclusion of the other modes.

In these studies a single wing tip sensor location was chosen to generate the feedback signal for all four store configurations. The selected location was found to yield the best average stability characteristics of all the wing locations. A pylon location was considered impractical, since this would require a new sensor on every store pylon. The wing sensor location has the advantage of being usable regardless of which pylon and store are being carried.

Frequency Domain Stability Results

Figures 4 and 5 summarize the active flutter control stable gain values and phase margins versus aircraft velocity for the cases studied. The results shown are for subsonic aerodynamics and sea level density. The use of supersonic aerodynamics had little effect on the stability margins.

Stability margins tend to improve with decreasing velocity and increasing structural damping. For each of the stores the stable gain values shown on the plots translate into gain margins of more than ±6 dB (factors of 2 and 1/2) for zero structural damping up to 730 knots, the maximum sea level capability of the aircraft with stores.

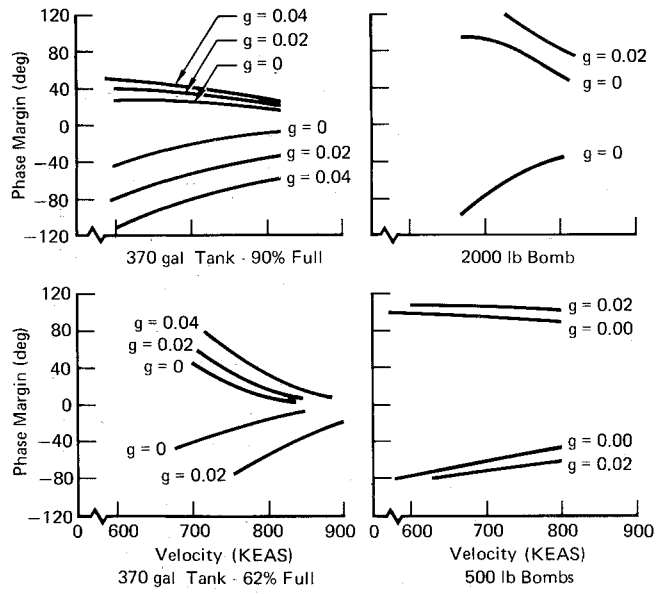

Fig. 5 Phase margins for compensated wing/store configurations—subsonic data.

This is a significant improvement over the indicated flutter onset velocities. Phase margins of ±60° or greater are shown for zero structural damping for each of the stores except the 370 gal tank. In that case, structural damping, $g = 0.02$, creates phase margins of approximately ±45° when 90% full and more than ±60° when 62% full.

The ever diminishing stability margins with increasing velocity infer that there is some velocity at which both phase and gain margins are zero. This velocity is the absolute limit velocity for the active flutter control scheme under consideration.

Decreasing air density degrades stability margins. The effect can be traced to aerodynamic damping which decreases with increasing altitude for a constant equivalent airspeed. Thus, similar to the effect of decreasing the structural damping, increasing altitude will decrease stability margins.

Control System Interaction

Integration of an active flutter control system with other flight control systems is desirable because of a reduction in both weight and cost compared with a dedicated flutter control system.

The general approach we have taken in the design of a flutter control system is to share selected portions of the existing aircraft flight control system. All of the elements incorporated in the loop for flutter control only are in the feedback branch (see Fig. 1) while those elements which are shared with the flight control system are in the forward loop. The flutter control feedback loop can thus be opened at subflutter velocities with no effect on the performance of the aircraft. A high pass filter is used to decouple the two systems for low frequency signals, such as pilot commands, when the loop is in operation.

Root locus runs were made to evaluate the interaction of the flutter control system with the Lateral/Directional Stability Augmentation System (SAS). The flight condition chosen for these runs was Mach 0.84 at sea level. The study configuration was that of the 370 gal tank 90% full.

Two sets of root loci were initially generated: one with the unmodified operational Lateral/Directional SAS and one with the SFCS secondary actuator replacing the existing servo-actuator and with the bandwidth of the aileron actuator extended to 10 Hz. Both sets indicated that the

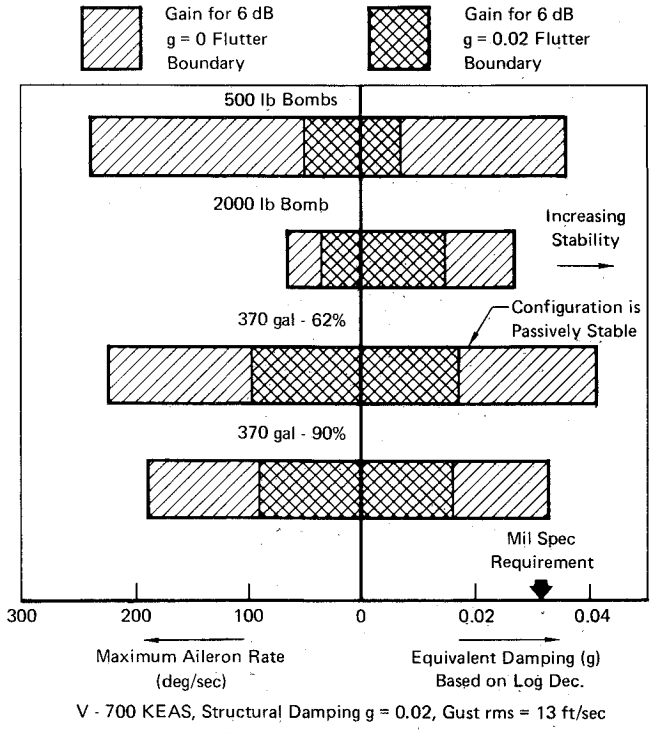

Fig. 6 Aileron rate and equivalent damping in flutter mode for wing/store study configurations.

system is highly damped. A third set of root loci then introduced the flutter control system as an inner control loop. The system was still very stable.

These runs illustrated that the flutter control system can be effectively decoupled from the flight control system, at least for fighter type aircraft with large frequency separation, even though the forward loop control elements are shared with the aircraft control system. Furthermore it shows that the wing modes considered here do not adversely affect stability.

There may, however, be significant effects on the flight control system design if the bandwidth of the common forward control loop is increased, as assumed in these studies. This was not apparent here because fuselage bending modes were not considered. Generally, sensors mounted in the fuselage will sense both rigid and elastic motion. Both types of signals may destabilize the control system and thus create divergent oscillations. An active flutter control system for an operational aircraft should thus be designed as an integrated package with all of the interacting control systems and all significant rigid and elastic modes considered simultaneously.

Control System Response Analyses

Time domain studies were conducted using the compensated control loops obtained from the frequency domain analyses. Time domain studies are useful not only in verifying the stability predictions of the frequency domain analysis but also in defining the hardware requirements for flutter control systems. In addition, the effect of nonlinear phenomena such as hydraulic rate limits, actuator deadspace, and aileron freeplay can be evaluated. Time domain studies thus enhance the realism of the simulation.

Linear Studies

The time domain studies were limited to four wing/store modes: the first three vibration modes and an aileron rotation mode. The number of modes was limited to avoid excessive computer time usage and to avoid integration errors which might arise from the presence of high frequency modes. For each of the wing/store configurations the basic flutter mechanism involved the interaction of the 2nd and 3rd modes.

Excitation of the time domain equations was achieved by using a gust force of the form

$$(10{,}000/2)\{1 - \cos[(2\pi)(\omega_F)t]\}\ \text{lb}$$

This represents the equivalent force excitation at the flutter frequency. ω_F, experienced by a minimum weight airplane flying through a typical thunderstorm at Mach 1.0, sea level conditions. The 10,000 lb amplitude was obtained by integrating under a power spectral density curve for a 13.38 ft/sec (rms) thunderstorm over the half power bandwidth of the flutter mode (8.0 to 8.7 Hz for the 90% full 370 gal tank).

Discrete gusts derived for the same thunderstorm at subflutter frequencies, as well as aircraft maneuver loads, produced rather mild system responses when compared with the flutter frequency gust.

Verification of System Stability

Time domain computer runs were made for each of the four compensated wing/store configurations at 700 knots, structural damping $g = 0.02$, sea level conditions. These runs verified system stability margins.

Aileron Rate and Displacement with No Limits

If it is assumed that the aileron response is not restricted in rate or displacement, maximum values can be read from the time history plots. Figure 6 summarizes maximum aileron actuator rates and the equivalent damping of the flutter mode obtained from the linear time domain computer runs. Data are shown for two gain settings giving 6 dB gain margins against the $g = 0$ and $g = 0.02$ passive flutter boundaries shown in Fig. 4.

For a given store the maximum aileron rate is proportional to the feedback gain. The aileron rate also varies linearly with the rms gust velocity, provided that the gust velocity is small when compared with the aircraft velocity. When these two facts are known a plot can be constructed showing aileron rate as a function of feedback gain and rms gust velocity. Figure 7 indicates a maximum

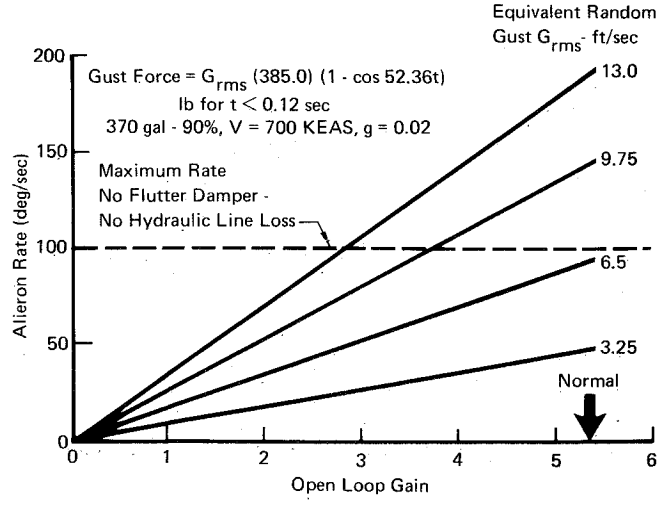

Fig. 7 Maximum aileron rate vs gust level and control system gain.

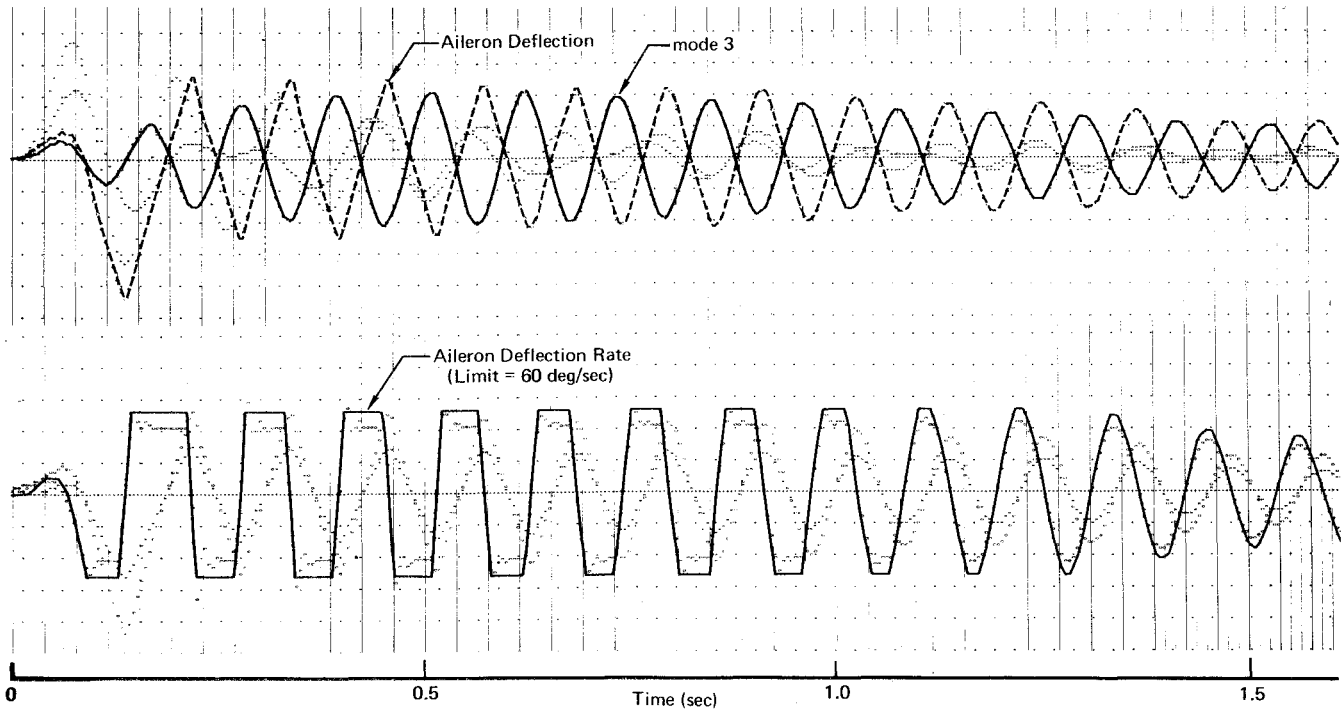

Fig. 8 Dynamic response plots illustrating effects of aileron actuator rate limit—60°/sec limit.

aileron rate of 100°/sec. This assumes that the flutter damper and line losses have been eliminated. The normal maximum rate capability at sea level is about 75°/sec. The figure also shows that strong vertical gusts cause actuator rate saturation. This raises the question of whether or not flutter control can be maintained during actuator rate saturation.

Nonlinear Studies

Stability with Actuator Limits

Deflection and rate limit cases were run with the 370 gal tank 90% full configuration. The 700 knots, structural damping $g = 0.02$, sea level, 13 ft/sec gust conditions were used in these time domain studies. Deflection limits of 10° and rate limits of both 100°/sec and 60°/sec were used.

Results from a run at 60°/sec are shown in Fig. 8. Active control is maintained, even though the actuators are rate saturated over a significant portion of each oscillation cycle. The actuator deflection limit was not encountered. The crucial factor was the net dissipation of airstream energy over each cycle. These results show that energy dissipation occurs even though the aileron displacement does not exactly conform to the command signal because of rate saturation. There is, however, some degradation in how fast the response is damped out, as shown by the effective damping coefficients, based on the logarithmic decrement

No Limits	$-g$ eff. = 0.033
100°/sec Limit	$-g$ eff. = 0.032
60°/sec Limit	$-g$ eff. = 0.023

Thus, to meet the military specification requirement of $g = 0.03$ in structural response (during flight through a typical thunderstorm) the actuator rate limit must be improved to at least 100°/sec.

Deadspace Evaluation

Deadspace, as defined in these studies, results from using control valve spools on the hydraulic actuator that are designed with overlap in order to eliminate leakage flow for zero-signal command. In time domain runs on the 370 gal tank 90% full the amplitude at the wing tip in the flutter mode is less than 0.3 in. and the aileron deflection less than 0.1° for deadspace overlap as large as 10% of full valve travel. The aileron actuator valve is designed for zero overlap.

Freeplay Evaluation

Freeplay arises because of "slop" in the force producer system outboard of the power actuator control valve. The net effect of freeplay is a constant time lag of the output. The maximum displacement is also reduced somewhat.

A test case for the 370 gal tank 90% full configuration with what amounted to a 3° lag freeplay effect was run on the time domain program. Stability was maintained with no significant performance degradation. The freeplay of the aileron has been undetectable in ground vibration tests and is much less than the military specification requirement of 1/30°.

System Safety Considerations

Reliability and Redundancy

Flight safety is a paramount design consideration for active flutter control systems, affecting the basic system complexity and redundancy and, thus, ultimately its total weight and cost. Some level of system redundancy is required because the catastrophic nature of the flutter phenomena demands continuous control during deep penetrations in the flutter region. The approach used in these studies was to use a minimum number of redundant control system components to guarantee a failure rate of less than one catastrophic failure (loss of aircraft) per million flight hours.

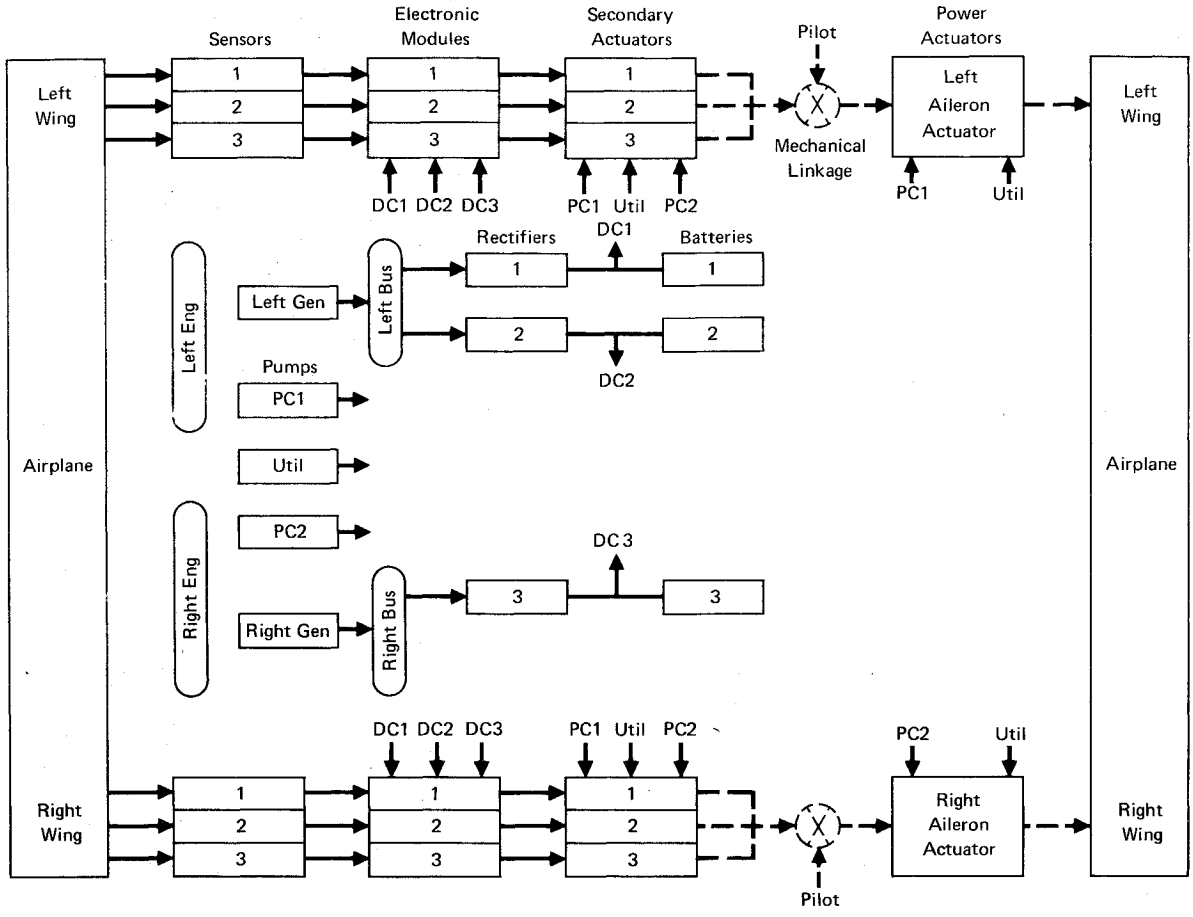

Fig. 9 Conceptual flow diagram for wing/store flutter control system.

Component Failure Rates

The failure rates of particular significance for active flutter control are shown below

	Component Failure Rate (per 10^6 hrs)
Aircraft a.c. Electrical Supply (Dual)	14.0
Engine Flameout (loss of hydraulic pumps)	30.0

If the active flutter control system included the full effects of only these two items the system failure rate would be 44 per million flight hours.

The failure of an active flutter control system during postflutter velocity flight infers loss of the aircraft, unless the flutter mechanism is disrupted. Thus, if a wing/store mechanism is being controlled, a high failure rate in the flutter control system might be acceptable if the stores were automatically ejected upon system failure. Ejection placards exist for nearly every flutter restricted store configuration because of the danger of impact of the store with the wing. Hence, to minimize catastrophic failures we considered elimination of high-failure-rate items.

Aircraft a.c. Electrical Supply

An active flutter control system requires both a.c. and d.c. power. Ordinarily, a.c. power is generated by two engine driven generators, and 28 V d.c. power is derived by rectifying the a.c. If both electrical generators fail (this occurs an average of 14 times every million flight hours) all power is cut off. To avoid losing this power, and hence control of flutter, an emergency 28 V d.c. battery supply could be incorporated in the active flutter control system. Direct current would be continuously available and any required a.c. power could be generated by new self-contained d.c. driven a.c. generators. The emergency battery supply would only have to function during the time it takes to slow the airplane to a subflutter velocity.

Engine Flameout

Engine flameout forces the hydraulic systems to rely on the stored energy in accumulators and power control reservoirs, and on engine rotary inertia. Engine rotary inertia provides a short-term decreasing hydraulic fluid flow rate.

It has been found in time domain runs with the 370 gal tank 90% full that flutter control can be maintained with aileron rate limits as low as 60°/sec, even though the limits are invoked as much as 50% of each cycle of motion. Calculations based on the 60°/sec case yield maximum flow requirements of 14 gal/min during the first second after the gust excitation. It takes the airplane about 20 sec after flameout to decelerate from 800 to 600 KEAS. At this time engine rotary inertia is still providing a hydraulic fluid flow rate of 20 gal/min. It can thus be concluded that flutter control can be maintained following engine flameout, even while the aircraft is flying through severe turbulence, provided that other aircraft hydraulic demands are small.

Voter Logic and Redundancy

In addition to a failure rate of less than one per million flight hours it is assumed that a practical flutter control specification will require that the first failure in the control system loop will cause no critical degradation of sys-

tem performance. A triply redundant electronic configuration is required to satisfy this one-fail-operate performance criterion, since it is not possible to recognize the good signal with only two signals to compare.

The pilot must be apprised of the failure to allow him to respond to the warning and reduce the speed of the aircraft. Off-line comparators, which operate when the difference of two signals is greater than a preset tolerance, are suitable for this monitoring requirement.

Design Uncertainties

MCAIR experience with fighter aircraft control systems indicates that phase margins of ±45° and gain margins of ±4.5 dB are realistic design criteria when analytical studies include control system nonlinearities. For linear analytical studies phase margins of ±60° and gain margins of ±6.0 dB can be justified. These stability margins have been considered as preliminary design guidelines in these flutter control studies.

Control System Uncertainties

The sensitivities to parametric variations in control system electronic components were determined for a typical flutter control system design. To guarantee a conservative evaluation, the following pessimistic tolerance values were used: ±10% on gains and ±20% on time constants. Each parameter of significance in the control loop was varied and the deviation of the open loop frequency response from nominal was determined in both gain and phase. The rss (root sum square) of these individual deviations was found to be less than 19° in phase and 1.5 dB in gain for frequencies up to 25 Hz. The rss infers that the error sources are independent and hence that the variance of the sum is the sum of the variances. These data indicate that a phase uncertainty of somewhat less than 20° should be easily achieved for the type of control systems being considered if quality components are used in the control loop electronics.

Experimental frequency response tests for the aileron power actuator show that maximum phase variation with signal size is only about 15° over the entire frequency range from 1 to 10 Hz. This effect is in addition to the previously defined rss electronic component phase uncertainties, that is $(19^2 + 15^2)^{1/2} = 24.2°$. This value is still well within the design guideline of ±45° phase margin when nonlinearities are included. The corresponding gain variation is on the order of 1.5 dB at 4 Hz, but near zero in the vicinity of the flutter frequencies at 8–10 Hz.

Aeroelastic System Uncertainties

As developed above, the electronic and hydraulic components of a flutter control system can be easily made to have a very small phase and gain uncertainty. In addition full-scale ground test data for both the electronic and hydraulic components can be credibly related to flight vehicle hardware.

The only unresolved uncertainties are those associated with the variable and unknown aeroelastic characteristics of the aircraft. There will always be unknowns in any practical wing/store configuration, not only because of analytical inadequacies but also because of unpredictables such as manufacturing tolerances on the stores, changes in wing-pylon-rack systems with normal operational use, and the inevitable provisions of Murphy's Law. One characteristic of the open loop frequency response function, however, can be used to eliminate virtually all of these aeroelastic system uncertainties in both wind tunnel models and operational flight vehicles. For flight below the flutter velocity, the Nyquist loop associated with the potentially unstable mode closes in a clockwise direction. At very low velocities, the plot may look like a "can of worms," and the significant modes may be difficult to determine. As the airspeed increases, however, the potential flutter mode becomes the single most predominant loop. As flutter is approached, the loop becomes progressively larger. It becomes infinite and the direction of closure changes to counter-clockwise at flutter onset. As the velocity increases further into flutter, the loop becomes progressively smaller.

The most significant characteristic of this transition is that the unstable postflutter loop is 180° out-of-phase with the stable subflutter loop. This characteristic has been observed in the computer program runs regardless of the number of potentially unstable modes or of the number of included degrees of freedom. A more detailed description of the Nyquist plot characteristics is given in Ref. 1.

Nyquist plots generated at subflutter velocities indicate the required phase change for flutter control. If the control system compensation is adjusted to locate the subflutter loop of interest so that its major axis is aligned along the positive real axis, the postflutter loop will be in the desired position, enclosing the origin with its major axis along the negative real axis.

For both wind tunnel and flight testing there is a need for sensible subflutter data, such as that just described, which will allow intelligent decisions to be made before proceeding into the postflutter region.

Flutter Control System Implementation

System Description

An argument has been made that a triply redundant electronic configuration would be required for a flutter control system. A conceptual flow diagram for such a system is shown in Fig. 9. The control loop is triply redundant from the sensors through the secondary actuators. It becomes a single path at the force-summing output shaft of the secondary actuator. The mechanical linkage which adds the pilot's commands to the flutter control system commands is part of this single path section. The loop becomes doubly redundant at the aileron actuator to complete the circuit.

Individual d.c. electrical sources and hydraulic power supplies are required for the operation of this flutter control system. The additional components shown in this figure are the sensors, electronic modules, secondary actuators, rectifiers and batteries. The batteries, which furnish the emergency d.c. power to the electronic modules, must be maintained by rigidly scheduled inspection and servicing to ensure their availability for backup.

Switching is provided in this system which would automatically connect the remaining good bus to the failed bus in the case of a single generator failure. This eliminates the need for battery power, except possibly during the switching process, for anything other than complete loss of aircraft a.c. power.

Weight Estimate

A weight estimate has been derived for the conceptual flow diagram of Fig. 9, using data from both the SFCS aircraft[7] and the F-4 CCV fighter studies. A system singular weight of 270 lb is estimated based on use of the lateral flight control loop, with the existing servo actuator replaced by the multiply redundant SFCS secondary actuator.

In future aircraft it is expected that flight control systems will use much more compact actuation concepts. This could reduce the estimated weight to approximately 200 lb, assuming that none of the weight for the primary actuation system is chargeable to the flutter control sys-

tem. If the flutter control system required separate dedicated components, the weight would be significantly greater.

Conclusions

These studies have shown that wing/store flutter can be stabilized with adequate stability margins using an active flutter control system which shares the aileron actuation hydraulics with the lateral control system. The flutter control system can be adapted to different store carriage configurations by adjusting the phase and gain characteristics of a generalized electronic compensation network. Control of a flutter mode can be maintained even though the hydraulic actuators are rate saturated for a significant portion of their stroking cycles. Before a flutter control system can be implemented on current aircraft actuator bandwidth should be extended and hydraulic flow rate increased. These improvements are within the current state-of-the-art. It is estimated that the flutter control system with triply redundant components will add about 270 lb to the aircraft weight.

References

[1]Triplett, W. E., "A Feasibility Study of Active Wing/Store Flutter Control," *Journal of Aircraft*, Vol. 9, No. 6, June 1972, pp. 438–444.

[2]Triplett, W. E., Kappus, H. P. F., and Landy, R. J., "Active Flutter Suppression Systems for Military Aircraft—A Feasibility Study," Tech. Rept. AFFDL-TR-72-116, Feb. 1973, Air Force Flight Dynamics Lab., Wright-Patterson Air Force Base, Ohio.

[3]Hodges, G. E., "Active Flutter Suppression—B-52 Controls Configured Vehicle," AIAA Paper 73-322, Williamsburg, Va., 1973.

[4]Noll, T. E. and Felt L. R., "Active Flutter Suppression—A Practical Application," National Aerospace Electronics Conference, Dayton, Ohio, May 1973.

[5]Ferman, M. A., Burkhart, T. H., and Turner, R. L., "First Quarterly Report for Conceptual Flutter Analyses," BuWeps Contract NOw 66-0298-C, Rept. E549, McDonnell Aircraft Co., St. Louis, Mo., March 1966; also Code AIR-604AI, Naval Air Systems Command, Dept. of Defense, Washington, D.C.

[6]Engquist, K. R., "Transonic Wind Tunnel Tests on a 13 Percent Semispan Model of the F-4E Airplane to Investigate Aerodynamic Loads on the Outboard Wing Panel and Leading Edge Slats," TR CAL-No. AA-4010-W-1, March 1970, Cornell Aeronautical Lab., Buffalo, N.Y.

[7]Hooker, D. S., Kisslinger, R. L., Smith G. R., and Smyth, M. S., "Survivable Flight Control System Interim Report No. 1 Studies, Analyses, and Approach," Tech. Rept. AFFDL-TR-71-20, May 1971, Air Force Flight Dynamics Lab., Wright-Patterson Air Force Base, Ohio.

NOVEMBER 1973 J. AIRCRAFT VOL. 10, NO. 11

An Omnidirectional Gliding Ribbon Parachute and Control System

William B. Pepper* and John R. Biesterveld†
Sandia Laboratories, Albuquerque, N. Mex.

An omnidirectional gliding, guided ribbon parachute and control system has been designed and tested. A 24-ft-(7.3-m)-diam ribbon parachute has been modified by incorporating four controllable glide flaps 90° apart at the skirt region and two roll flaps 180° apart. The design includes a control system consisting of a remote command transmission site and an on-board sensing and receiving station and control line operation. Four drop tests of a 2600-lb (1179-kg) test vehicle have demonstrated that the system is feasible if the parachute is carefully modified, if glide flaps are provided for omnidirectional control, and if an on-board sensor is used for roll control.

Introduction

RIBBON parachutes[1] are often used to control down time, impact velocity and impact attitude of bombs. The accuracy for parachute retarded delivery of stores is about an order of magnitude worse than a free-fall delivery due to wind drift and drag-area variations. The three sigma dispersion is about 100 mils based on trajectory length for parachute retarded weapons. This dispersion does not include release point error or errors in wind prediction.

It has been demonstrated[2-4] that a ribbon parachute will glide with a lift-to-drag ratio of about 1/3 if the skirt region is lined with solid cloth. Only two glide flaps in the skirt region of the parachutes were used on these original, similar tests.[2,3] It was believed desirable to introduce four glide flaps 90° apart at the parachute skirt so that the vehicle could be glided in any direction without rolling the system appreciably.

The data from four drop tests of a 2600-lb (1179-kg) vehicle released at 130 knots (67 m/s) true air speed at a 13,000-ft (3962-m) altitude to evaluate the four-flap system for guiding a 24-ft-(7.3)-diam ribbon parachute are presented herein.

History

Development work on the feasibility of guiding a store by means of a ribbon parachute began at Sandia Laboratories in early 1969. These early drop tests, along with wind tunnel tests,[5] established that a ribbon parachute with a lined skirt could achieve a glide ratio‡ of 1/3 if an opening of proper size was introduced into the lined portion. Subsequent tests showed that simple and reliable

Presented as Paper 73-486 at the AIAA 4th Aerodynamic Deceleration Systems Conference, Palm Springs, Calif., May 21–23, 1973. This work was supported by the U.S. Atomic Energy Commission and the U.S. Air Force Weapons Laboratory, Kirtland Air Force Base, N. Mex.

Index categories: Aircraft Deceleration Systems; Navigation, Control and Guidance Theory; Spacecraft Navigation, Guidance, and Flight-Path Control Systems.

*Member of the Technical Staff, Aerodynamics Projects Department. Associate Fellow AIAA.

†Staff Assistant Technical, Upper Atmospheric Projects Department.

‡Lift/drag.